J. Am. Soc. Mass Spectrom. (2018) 29:1036–1043
DOI: 10.1007/s13361-018-1908-z

RESEARCH ARTICLE

Microdroplets Accelerate Ring Opening of Epoxides

Yin-Hung Lai, Shyam Sathyamoorthi, Ryan M. Bain, Richard N. Zare

Department of Chemistry, Stanford University, Stanford, CA 94305, USA

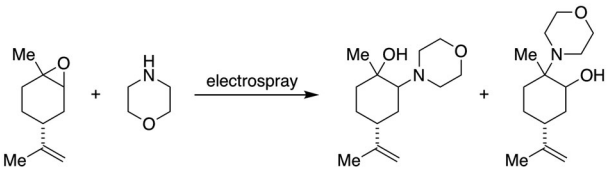

Abstract. The nucleophilic opening of an epoxide is a classic organic reaction that has widespread utility in both academic and industrial applications. We have studied the reaction of limonene oxide with morpholine to form 1-methyl-2-morpholino-4-(prop-1-en-2-yl) cyclohexan-1-ol in bulk solution and in electrosprayed microdroplets with a 1:1 *v*/*v* water/methanol solvent system. We find that even after 90 min at room temperature, there is no product detected by nuclear magnetic resonance spectroscopy in bulk solution whereas in room-temperature microdroplets (2–3 μm in diameter), the yield is already 0.5% in a flight time of 1 ms as observed by mass spectrometry. This constitutes a rate acceleration of ~ 10^5 in the microdroplet environment, if we assume that as much as 5% of product is formed in bulk after 90 min of reaction time. We examine how the reaction rate depends on droplet size, solvent composition, sheath gas pressure, and applied voltage. These factors profoundly influence the extent of reaction. This dramatic acceleration is not limited to just one system. We have also found that the nucleophilic opening of *cis*-stilbene oxide by morpholine is similarly accelerated. Such large acceleration factors in reaction rates suggest the use of microdroplets for ring opening of epoxides in other systems, which may have practical significance if such a procedure could be scaled.

Keywords: Microdroplet, Electrospray ionization, Reaction acceleration, Epoxide ring opening, Microparticle imaging velocimetry

Received: 29 November 2017/Revised: 18 January 2018/Accepted: 29 January 2018/Published Online: 22 March 2018

Introduction

Morpholine is a heterocycle that is ubiquitous in molecules of clinical and industrial interest [1]. One widely used method for the introduction of morpholine into these compounds is through a nucleophilic ring opening of epoxides [2]. In bulk, the opening of limonene oxide with morpholine is reported to occur (Fig. 1a) only at elevated temperatures (60–70 °C) with extended reaction times (16–48 h) [3].

Corroborating this, in our own hands, no conversion to product is noted at room temperature by ^{1}H NMR, even after 1.5 h. In sharp contrast, when a room-temperature solution of morpholine and limonene oxide in 1:1 *v*/*v* MeOH/H_2O was pumped through a homebuilt electrospray ionization (ESI) source to produce charged microdroplets (Fig. 2), the ring-opened product(s) is observed on the millisecond timescale. A representative ESI spectrum depicting the microdroplet reaction between limonene oxide and morpholine is presented in Fig. 1b. It should be noted that morpholine could also conceivably add to the olefin of limonene oxide. However, collision-induced dissociation (CID) of the product ions (*m*/*z* 240.1950) showed a clear loss of water, indicating the existence of a hydroxyl group (Fig. 1c). Thus, we believe that the addition of morpholine to the olefin is not the major pathway.

Although it is well established that microdroplets provide unique environments for a variety of chemical reactions, the mechanisms underlying this phenomenon are not fully understood [4–6]. While microdroplet research was initiated as a means of monitoring bulk processes, it soon became apparent that dramatic rate accelerations of reactions occurred within the droplet [7–16]. One of the first reports of accelerated reactions

Yin-Hung Lai, Shyam Sathyamoorthi, and Ryan M. Bain contributed equally.

Electronic supplementary material The online version of this article (https://doi.org/10.1007/s13361-018-1908-z) contains supplementary material, which is available to authorized users.

Correspondence to: Richard Zare; *e-mail:* zare@stanford.edu

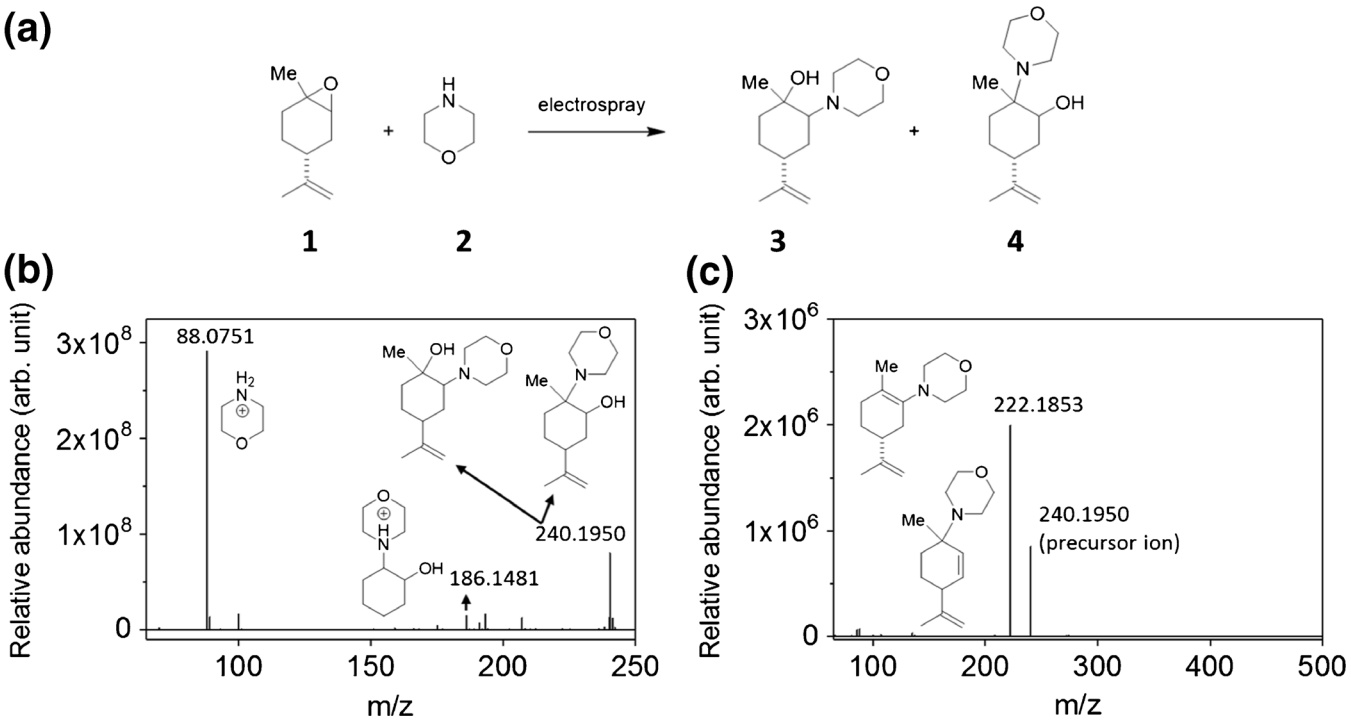

Figure 1. **a** Nucleophilic opening of limonene oxide (1) with morpholine (2) to produce products (3) and (4). **b** Representative ESI spectrum (positive mode) for the reaction of limonene oxide with morpholine in microdroplets. Protonated morpholine (*m/z* 88), protonated internal standard (*m/z* 186), and protonated product(s) (*m/z* 240) were observed. **c** CID-MS^2 of the mass-selected ion at *m/z* 240.1950

in electrosprayed droplets was by Lee et al. in 2015 where two electrospray droplet streams (each containing separate reagents) were fused together, allowing kinetic measurements on the millisecond timescale [17]. Reaction kinetics in these droplets were found to be significantly faster than the corresponding bulk-phase kinetics for a variety of reactions and suggested that there was inherent reactivity at the surface of the electrospray droplet. This rate acceleration has been preliminarily attributed to a variety of factors, including the increased surface area-to-volume ratio in the droplet, fast mixing caused by two-dimensional diffusion, increased reagent concentrations at the surface because of continuous solvent evaporation and/or hydrophobic segregation, decreased solvation shell energy [18–22], and large electric fields at the air-droplet interface [6, 23]. It is our hope that a fundamental understanding of the mechanisms of droplet acceleration will aid in the future translation of these microscale reactions into macro-processes of synthetic utility [16, 24, 25].

The size and speed of a microdroplet, its solvent constituency, and the voltage with which it is electrosprayed are all factors that are predicted to have profound effects on reaction kinetics within the droplet [6]. As the droplet radius decreases,

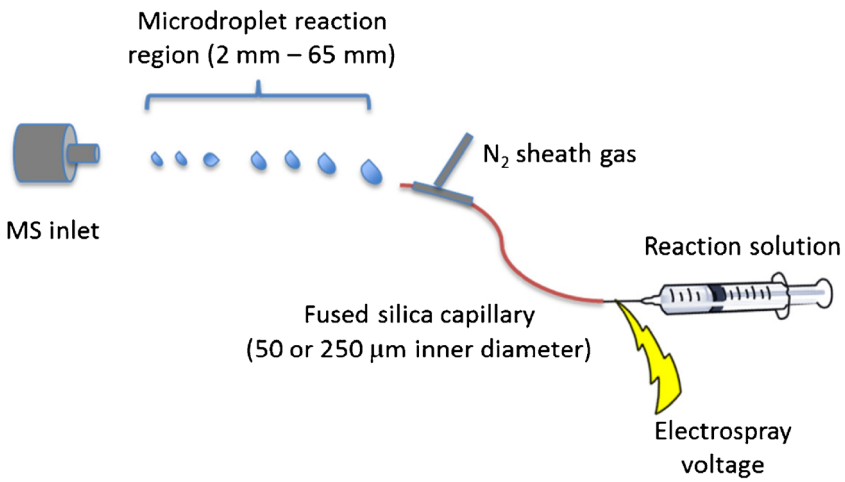

Figure 2. Schematic of the experimental setup for conducting and monitoring the nucleophilic opening of limonene oxide with morpholine in charged microdroplets produced by electrospray ionization

its surface area-to-volume ratio increases. With more surface sites for reagents to dwell, the probability of intermolecular collisions increases. Indeed, taken to an extreme, a three-dimensional reaction in bulk is nearly confined to two dimensions in a microdroplet, allowing for exceedingly rapid interactions between starting materials. This phenomenon has been termed "compartmentalization of reagents" on the surface of the microdroplet. However, methods that decrease the size of droplets, such as increasing sheath gas pressure, may also increase the speed. As the reaction time in a droplet is directly related to the flight time from source to detector, the speed of a "droplet reactor" is a critical parameter that affects the conversion of starting material to product. By systematically varying these parameters and tracking the formation of the product, we hoped to unravel these competing effects, using the nucleophilic opening of limonene oxide with morpholine as a model reaction (Fig. 1a).

Experimental Section

Online Electrospray Ionization Mass Spectrometry

Online electrospray ionization mass spectrometry was performed using a homebuilt electrospray source as described in [26]. In our system, we premixed the reagents and sprayed the mixed solution toward the mass spectrometer. A positive ion mode was used to detect ions with a positive voltage of + 5 kV applied to the syringe (unless otherwise stated) which pumped the reaction solution at a flow rate of 5 μL/min through silica tubing (Polymicro Technologies) with a coaxial sheath gas flow (N_2 at 120 psi, unless otherwise stated). The ion transfer capillary temperature was 275 °C, the capillary voltage was kept at 44 V, and the tube lens voltage was 60 V. The spray distance (i.e., the distance between the MS inlet and the tip of the spray source) was varied between 2 and 65 mm. An LTQ Orbitrap XL Hybrid Ion Trap-Orbitrap mass spectrometer (Thermo Fisher Scientific, San Jose, CA) was used for the detection of ions.

Microparticle Imaging Velocimetry

The method utilizing micro-PIV to measure size and speed of microdroplets has been described in detail elsewhere [12]. Micro-PIV is an offline experiment that was performed with the same electrospray source but using a grounded piece of metal in place on the ion transfer capillary. An external voltage source (Bertan, Valhalla, NY) and a syringe pump (Harvard Apparatus, Cambridge, MA) were also used. Two-pulsed second harmonic Nd:YAG lasers (Minilase II, New Wave, Fremont, CA, and DCR-11, Spectra Physics, Santa Clara, CA, λ = 532 nm) with additional optics were used to set up the illumination system for imaging the spray. Pulse durations (FWHM) and jitters for Minilase II and DCR-11, which allow us to "freeze" droplets, were 5 ± 1 and 25 ± 10 ns, respectively. The setup for electrospray was fitted into an inverted microscope using a 5x magnification, NA = 0.15 objective with 13.6 mm free working distance (Plan-Neofluar, AxioVert 135, Carl Zeiss Microscopy, Thornwood, NY). An interline CCD camera with the double-image feature (MicroMAX DIF, Princeton Instruments, Trenton, NJ) was used for rapid image acquisition (1 μs integration time per frame). The final image, recorded by the CCD, can be estimated as a convolution of the point response function and the particle diameter. Thus, there is a limit of detection of droplet size (1.3 μm, 4 × 4 pixels on the imaging plane) caused by the point response function that depends on both the optical system and the wavelength of light being used for imaging. In other words, all droplets of physical diameters of 1.3 μm or less will cover an area of about 4 × 4 pixels on the imaging plane. The average size of droplets was estimated from the average pixels that microdroplets occupy on the imaging plane. By regulating the time interval between two laser pulses (ΔT = 500–1000 ns), two consecutive frames showing the displacement of microdroplets were obtained. The average speed of droplet was calculated by dividing the displacement with the time interval.

Results and Discussion

Figure 3 presents a plot of the reaction progress as a function of time, for fused silica capillaries of 50 and 250 μm inner diameters (i.d.). We systematically varied the distance between the tip of the spray source and the inlet of the mass spectrometer (MS) while measuring the intensity of product ion relative to that of an internal standard (2-morpholino-cyclohexan-1-ol). Using a calibration curve (Fig. S1 in the Supplementary Material), the concentration of the product could be determined. The distance from spray source to detector is directly related to the reaction time inside the droplet [17]. By

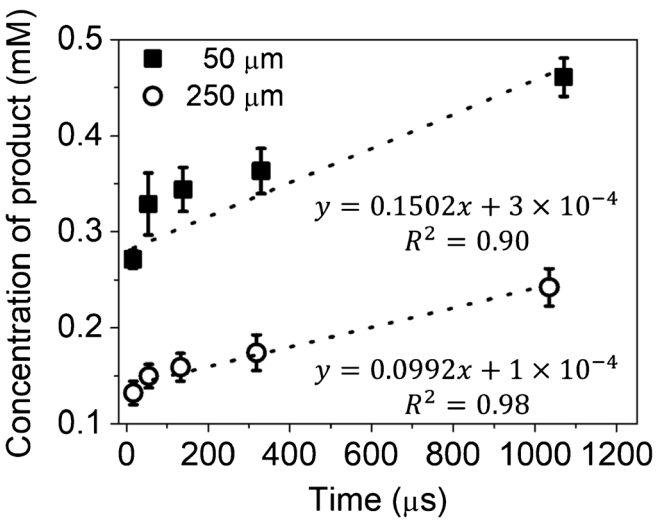

Figure 3. Concentration of the product (3) or (4) over time for 50 μm (solid squares) and 250 μm (open circles) i.d. fused silica capillaries. The solvent was 1:1 *v/v* MeOH/H_2O in this experiment. See Fig. S2 in the Supplementary Material for the raw data from which this plot was generated. Please note that here and elsewhere, error bars correspond to one standard deviation of a data set where $n = 3$, and the circle shown is the mean

measuring the average speed of microdroplets at a given distance (see "Experimental Section" and Supplementary Material), the flight time of the droplet could be determined. Improved reaction progress is evident in Fig. 3 as the flight time of the droplet increases.

As noted in Fig. 1a, two possible ring-opened products are possible in this reaction. We have thus also examined the opening of *cis*-stilbene oxide with morpholine (Fig. 4). In this simpler system, where only one ring-opened product is possible due to symmetry of the starting epoxide, we see a similar trend as in Fig. 3. These results suggest that the reactions occur in the microdroplet environment as the droplets travel toward the mass spectrometer inlet and are not the result of simply a microscale bulk process that is subsequently detected with the high sensitivity of the Orbitrap mass spectrometer. Product formation is also not the result of a reaction inside the heated inlet of the mass spectrometer. If this were the major source of product formation, then we would not have observed the product yield change as a function of distance between the spray source and the inlet of the mass spectrometer (Fig. 3). As the MS capillary inlet temperature changes from 130 to 275 °C, there is little fluctuation in the yield of ring-opened products 3 and 4 (Fig. 5).

To approximate a factor of rate acceleration for the opening of limonene oxide with morpholine, we must make two assumptions about the bulk reaction process: 1. In 90 min, approximately 5% of product is formed in bulk solution; a conservative estimate (which is likely an overestimate) for the detection in ^{1}H NMR spectroscopy is 20:1 relative to the most abundant species. The limit of detection of an NMR instrument depends on both the intrinsic properties of molecules and the instrument design, such as the magnetogyric ratio of the spin

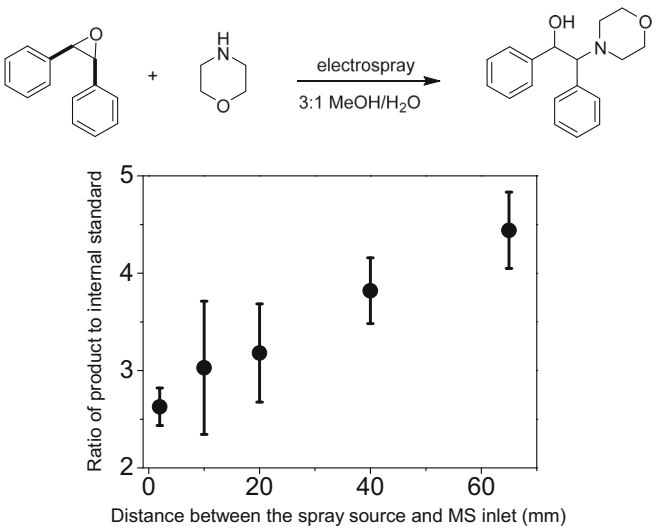

Figure 4. The nucleophilic opening of *cis*-stilbene oxide with morpholine in electrosprayed droplets. Improved reaction progress is evident as the distance between the spray source and MS inlet increases, which corresponds to increase of flight time of the droplet. Error bars correspond to one standard deviation of a data set where $n = 3$, and the circle shown is the mean

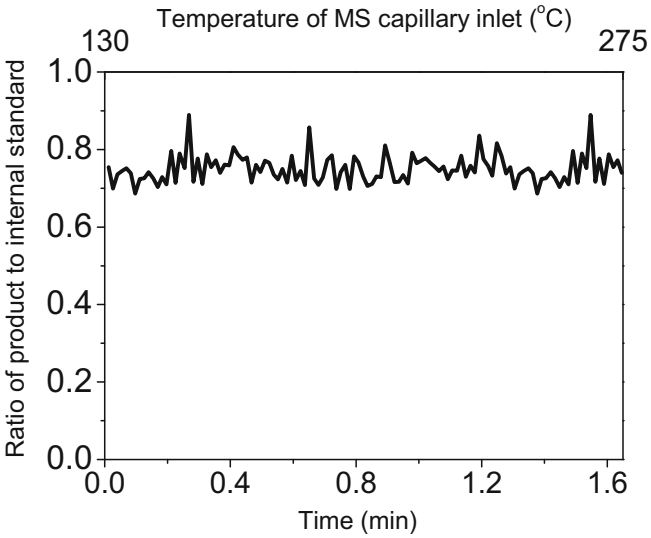

Figure 5. The yield of ring-opened products 3 and 4 (the ratio of the intensity of product relative to that of internal standard) varies little as the capillary inlet temperature increases from 130 to 275 °C over a period of 1.6 min

and the strength of static field [27]. As a general rule, for quantitation in NMR, the detection limit of a species is set at 5%. 2. The formation of product during this time is in the "linear region" of the second-order kinetics [28] of the overall process. In this linear region, the reaction follows zero-order kinetics because large excesses of both reagents exist. The rate of formation is then simply the total amount of product formed divided by the total reaction time elapsed. Based on these assumptions, the rate of formation of product in bulk is calculated to be 9×10^{-7} ms^{-1} while in the microdroplet environment, the rate constants are 1.5×10^{-1} and 9.9×10^{-2} ms^{-1} for a capillary inner diameter (i.d.) of 50 and 250 μm, respectively (Fig. 3). Thus, the reaction progresses approximately 10^5 times faster in the microdroplet compared to that in bulk solution.

For all reaction times measured, the conversion to product is increased for microdroplets produced from the 50-μm fused silica capillary relative to those from the 250-μm capillary (Fig. 3). The average droplet size produced from these two capillaries was measured using micro-PIV. Figure 6 shows images of microdroplets produced by the two spray sources. A typical electrospray is composed of three distinct regions, namely, the Taylor cone, jet, and plume [29–32]. Electrospray from a 250-μm-i.d. capillary has relatively clear Taylor cone and jet regions; a cloudy plume is observed with the 50-μm-i.d. capillary. As hypothesized, droplets produced from 50-μm capillaries (average size ca. 2.0 μm ± 0.3 μm) are consistently smaller than those from 250-μm capillaries (average size ca. 3.1 μm ± 0.4 μm). From these measured sizes, knowing that our infusion rate into the spray sources was fixed (5 μL/min), and making the simplifying assumption that the microdroplets are spherical, it follows that the ratio of the total surface area from the 50-μm capillary droplets to that from the 250-μm capillary droplets is 1.6. Electrospray from 50-μm capillaries has smaller initial droplets; at a constant spray voltage (+ 5 kV),

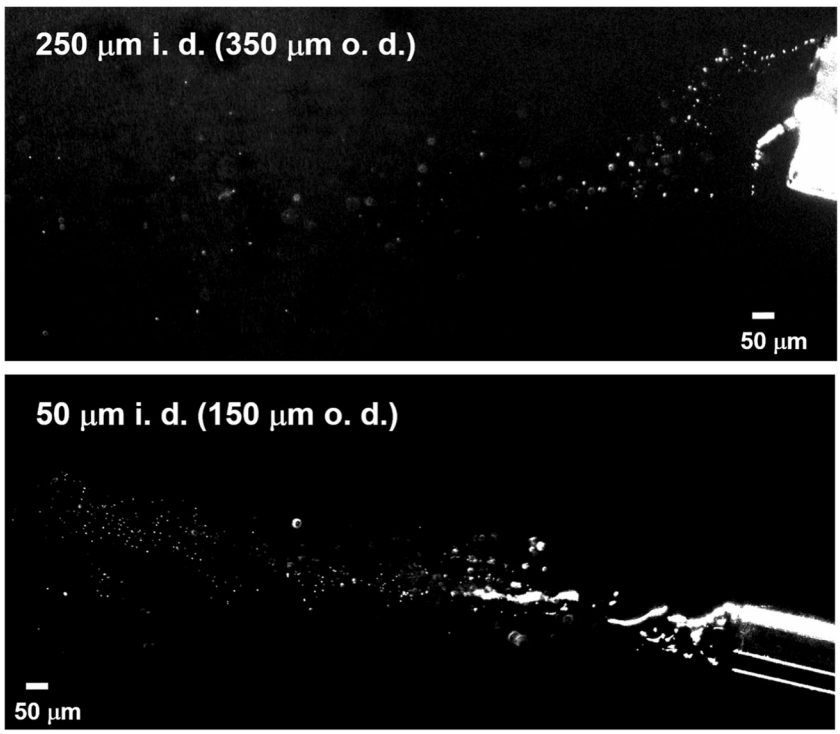

Figure 6. Microparticle imaging of droplets produced by 50 and 250 μm i.d. fused silica capillaries. Average droplet sizes generated from 50 and 250 μm capillaries were 2.0 μm ± 0.3 and 3.1 μm ± 0.4 μm, respectively. The solvent used was 1:1 *v/v* MeOH/H_2O. Microdroplets were generated from a 1:1 mixture of MeOH/H_2O with a sheath gas pressure (N_2) of 120 psi and a flow rate of 5 μL/min

the surface charge density is thus expected to be higher, which leads to a higher incidence of Coulomb fission [33]. The inverse relationship between droplet size and organic reaction yield has been previously described for the formation of a fluorescent imine [34]. In this previous study, droplets were produced via microfluidic emulsification and had sizes between 8 and 34 μm. It should be noted that our study is the quantitative illustration of this phenomenon in droplets produced by electrospray ionization; furthermore, the microdroplets produced in our study are approximately an order of magnitude smaller than those produced through microfluidic methods. For a fixed sheath gas pressure and spray voltage, there is thus a clear correlation between reduced droplet radius and increased reaction yield.

Size is not the only factor that affects reaction yield; solvent also has a profound influence on opening of limonene oxide by morpholine. As the ratio of methanol to water increases from 1:1 to 19:1, there is a marked decrease in formation of product (Fig. 7). At a fixed sheath gas pressure of 60 psi, the average droplet sizes in 1:1 and 9:1 (MeOH/H_2O, *v/v*) are 9.5 and 4.2 μm, respectively. As we increase the percentage of MeOH, the average droplet size drops (to 2.8 μm for pure MeOH). Product yield continues to decrease until pure MeOH is used. It appears that the presence of water is beneficial for the nucleophilic ring opening of limonene oxide in microdroplets, a phenomenon that has previously been described in bulk, where adding equivalents of water led to dramatically higher yields of ring-opened product [3]. Once pure methanol is used, the trend no longer holds and this is likely due to the contribution of the increased surface area-to-volume ratio given by the smaller droplets. The contribution of droplet size to the reaction rate then overcomes the reduced conversion in pure methanol that is seen in bulk. Please note that the ionization efficiency of the

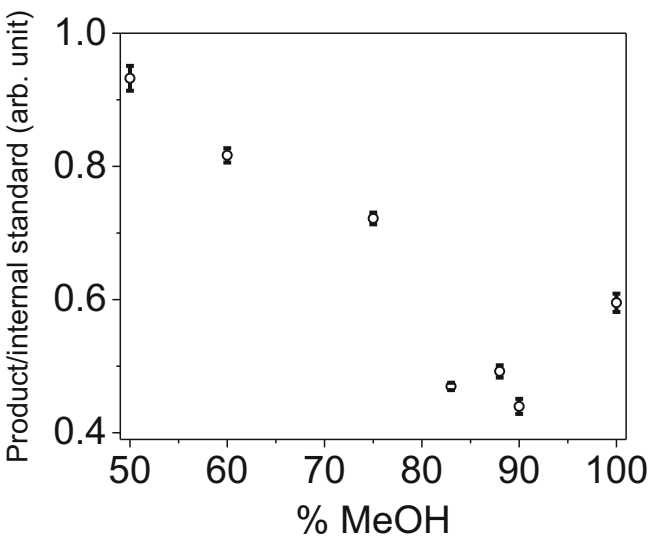

Figure 7. Effect of solvent on the yield of ring-opened products 3 and 4. Please note that the product/internal standard ratio was not converted to absolute product concentrations because the calibration curve was done using 1:1 *v/v* MeOH/H_2O and does not apply to different solvent compositions. Droplets were generated at a sheath gas pressure of 120 psi and a solvent flow rate of 5 μL/min

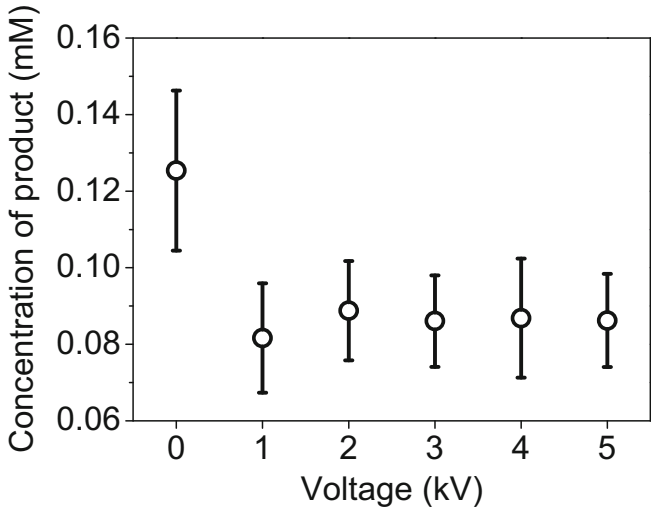

Figure 8. Dependence of product concentration (Fig. 1a, species 3 and 4) on applied voltage at a fixed distance of 10 mm between the spray source and the mass spectrometer inlet for a 250-μm-i.d. capillary. Droplets were generated from a 1:1 solution of MeOH/H_2O at a N_2 sheath gas pressure of 120 psi and a syringe pump flow rate of 5 μL/min. The error bars represent one standard deviation for three measurements

product does not change significantly as the percentage of methanol increases (Fig. S3, Supplementary Material).

While increased voltage may contribute to a higher incidence of Coulomb fission and may in part account for the increased yield seen in electrospray from the 50-μm-i.d. capillary, curiously, Fig. 8 shows that applying a positive voltage in general has a detrimental effect on ring opening of limonene oxide. Examining the formation of product in electrospray from a 250-μm-i.d. capillary at increasing positive voltages (from 0 kV (sonic spray ionization) [35, 36] to + 5 kV) reveals a clear "on/off" effect, where any amount of positive voltage impairs reaction progress. This observation is perhaps additional evidence that product formation is the result of a microdroplet reaction. The existence of positive voltage presumably enriches the droplet with protons [37], protonating morpholine and hence attenuating its nucleophilicity. This behavior contrasts with the work of Mueller, Badu-Tawiah, and Cooks, who showed that in basic droplets, the polarity of the applied voltage was not a significant factor [25]. Rather, in their base-catalyzed condensation reaction, both positive and negative applied voltage produced more product than in the corresponding experiment without any external voltage. In their case, it is likely that the voltage applied solely contributes to Coulomb fission, creating smaller droplets without altering the pH at the surface of a 9×10^{-2} M potassium hydroxide droplet. Banerjee and Zare have demonstrated an increased reaction rate with greater positive voltage in the acid-catalyzed formation of isoquinoline and substituted quinolines in microdroplets [10]. As these reactions are known to be acid-catalyzed in bulk, it is likely that a combination of pH and droplet size played a significant role in product formation.

Having considered the effects of droplet size, solvent composition, and spray voltage on reaction progress, we next sought to elucidate the effect of droplet speed. As droplet speed is directly related to reaction time, we hypothesized that faster-moving droplets would exhibit diminished conversion to product. Simply reducing the inner diameter of the spray source capillary has little effect on droplet speed, as measured using micro-PIV (see Fig. S4 in the Supplementary Material). Average droplet speeds at different distances between the spray source and MS inlet were similar for both 50- and 250-μm-i.d. capillaries. We found that the average droplet speed increases as the spray source is brought closer to the inlet from 65 to 2 mm. Varying the N_2 sheath gas pressure, however, has a

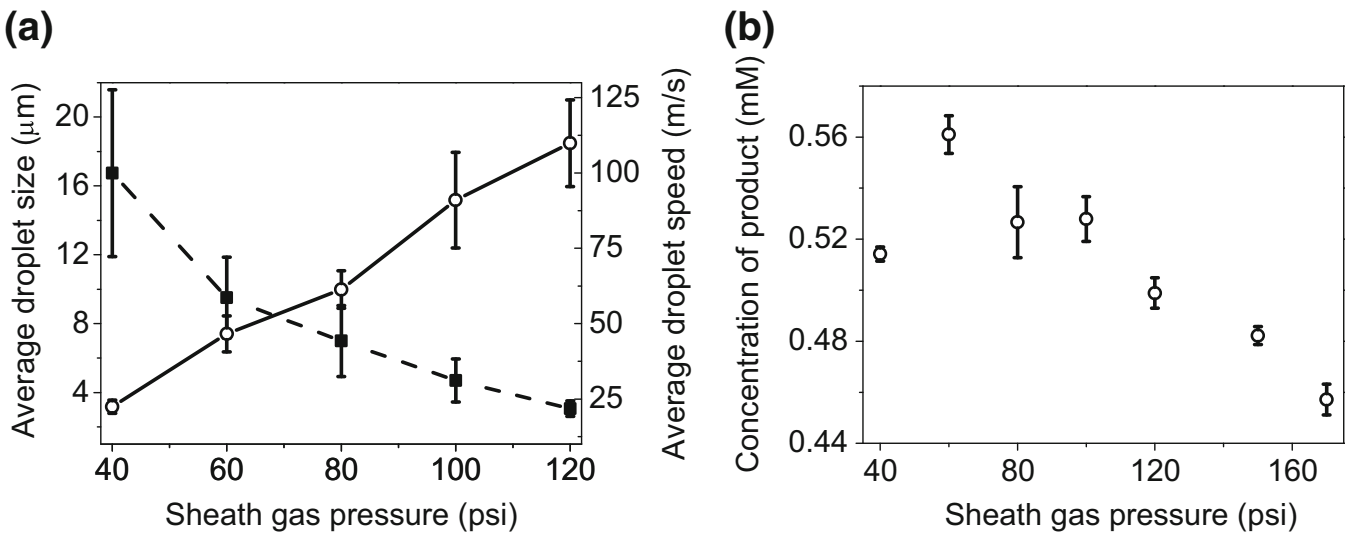

Figure 9. The effect of varying the sheath gas pressure on **a** average droplet size (solid squares connected with a dashed line) and average speed (open circles connected with a solid line) and **b** product (Fig. 1a, species 3 and 4) formation. In a 250 μm i.d. capillary, droplets were generated from a 1:1 solution of MeOH/H_2O at a N_2 sheath gas pressure of 120 psi and a syringe pump flow rate of 5 μL/min. The error bars represent one standard deviation based on three measurements

dramatic effect on both droplet speed and size. As sheath gas pressure is systematically increased from 40 to 120 psi, the average droplet size diameter decreases from 17 to 3.1 μm (Fig. 9a and Fig. S5 in the Supplementary Material). At the same time, the average droplet speed increases from 22 m/s at 40 psi to 110 m/s at 120 psi. Thus, changing the sheath gas introduces two competing effects in the droplet reaction. Over the range of pressures tested, the reaction surface area is increased by a factor of 5.5, but the reaction time is decreased by a factor of 4.9. This trade-off is reflected in the plot of product formation vs. sheath gas pressure (Fig. 9b). When the sheath gas pressure is varied from 40 to 170 psi, the conversion to product in the microdroplet increases up to a pressure of 60 psi and then subsequently decreases. This rise and fall is consistent with our expectation that product yield is a convolution of two competing effects [38].

Concluding Remarks

We have demonstrated a dramatic rate acceleration of the nucleophilic ring opening of both limonene oxide and *cis*-stilbene oxide with morpholine in microdroplets relative to that in bulk solution. We have conducted an in-depth mechanistic analysis of this process by examining the effects of size, speed, spray voltage, and solvent on reaction progress. For a fixed spray voltage and sheath gas pressure, decreasing the size of the microdroplet dramatically increases conversion to product. Increasing the sheath gas pressure from 40 to 170 psi simultaneously decreases the size and increases the speed of the microdroplet. These two offsetting effects lead to a complex dependence of reaction performance on sheath gas pressure, with an initial increase in product yield followed by a sharp decrease. Positive spray voltage decreases reaction performance, likely by reducing the nucleophilicity of morpholine. Solvent trends "in-droplet" mirror those seen in bulk, with increased amounts of water having a beneficial effect on product formation. It is our hope that enhanced reaction rates in microdroplets will provide in the future macroscale conversions for synthetic preparations.

Acknowledgments

We gratefully acknowledge the Air Force Office of Scientific Research through Basic Research Initiative grant (AFOSR FA9550-16-1-0113) for supporting this work.

References

1. Wijtmans, R., Vink, M.K., Schoemaker, H.E., van Delft, F.L., Blaauw, R.H., Rutjes, F.P.: Biological relevance and synthesis of C-substituted morpholine derivatives. Synthesis. **5**, 641–662 (2004)
2. Saddique, F.A., Zahoor, A.F., Faiz, S., Naqvi, S.A.R., Usman, M., Ahmad, M.: Recent trends in ring opening of epoxides by amines as nucleophiles. Synth. Commun. **46**, 831–868 (2016)
3. Goralski, C.T., Hasha, D.L., Singaram, B., Steiner, D.: Scale-up of the preparation of (1R,2R,4S)-1-methyl-4-(1-methylethenyl)-2-(4-morpholinyl)cyclohexanol. Org. Process. Res. Dev. **11**, 776–779 (2007)
4. Lee, J.K., Banerjee, S., Nam, H.G., Zare, R.N.: Acceleration of reaction in charged microdroplets. Q. Rev. Biophys. **48**, 437–444 (2015)
5. Li, Y., Yan, X., Cooks, R.G.: The role of the Interface in thin film and droplet accelerated reactions studied by competitive substituent effects. Angew. Chem. Int. Edit. **55**, 3433–3437 (2016)
6. Yan, X., Bain, R.M., Cooks, R.G.: Organic reactions in microdroplets: reaction acceleration revealed by mass spectrometry. Angew. Chem. Int. Edit. **55**, 12960–12972 (2016)
7. Augusti, R., Chen, H., Eberlin, L.S., Nefliu, M., Cooks, R.G.: Atmospheric pressure Eberlin transacetalization reactions in the heterogeneous liquid/gas phase. Int. J. Mass Spectrom. **253**, 281–287 (2006)
8. Bain, R.M., Pulliam, C.J., Ayrton, S.T., Bain, K., Cooks, R.G.: Accelerated hydrazone formation in charged microdroplets. Rapid Commun. Mass Spectrom. **30**, 1875–1878 (2016)
9. Bain, R.M., Pulliam, C.J., Cooks, R.G.: Accelerated Hantzsch electrospray synthesis with temporal control of reaction intermediates. Chem. Sci. **6**, 397–401 (2015)
10. Banerjee, S., Zare, R.N.: Syntheses of isoquinoline and substituted quinolines in charged microdroplets. Angew. Chem. Int. Edit. **54**, 14795–14799 (2015)
11. Girod, M., Moyano, E., Campbell, D.I., Cooks, R.G.: Accelerated bimolecular reactions in microdroplets studied by desorption electrospray ionization mass spectrometry. Chem. Sci. **2**, 501–510 (2011)
12. Jansson, E.T., Lai, Y.-H., Santiago, J.G., Zare, R.N.: Rapid hydrogen–deuterium exchange in liquid droplets. J. Am. Chem. Soc. **139**, 6851–6854 (2017)
13. Mortensen, D.N., Williams, E.R.: Ultrafast (1 μs) mixing and fast protein folding in nanodrops monitored by mass spectrometry. J. Am. Chem. Soc. **138**, 3453–3460 (2016)
14. Mortensen, D.N., Williams, E.R.: Investigating protein folding and unfolding in electrospray nanodrops upon rapid mixing using theta-glass emitters. Anal. Chem. **87**, 1281–1287 (2015)
15. Bain, R.M., Sathyamoorthi, S., Zare, R.N.: "On-droplet" chemistry: the cycloaddition of diethyl azodicarboxylate and quadricyclane. Angew. Chem. Int. Edit. **56**, 15083–15087 (2017)
16. Jacobs, M.I., Davies, J.F., Lee, L., Davis, R.D., Houle, F.A., Wilson, K.R.: Exploring chemistry in micro-compartments using guided droplet collisions in a branched quadrupole trap coupled to a single droplet, paper spray mass spectrometer. Anal. Chem. **89**, 12511–12519 (2017)
17. Lee, J.K., Kim, S., Nam, H.G., Zare, R.N.: Microdroplet fusion mass spectrometry for fast reaction kinetics. Proc. Natl. Acad. Sci. U. S. A. **112**, 3898–3903 (2015)
18. Aragonès, A.C., Haworth, N.L., Darwish, N., Ciampi, S., Bloomfield, N.J., Wallace, G.G., et al.: Electrostatic catalysis of a Diels–Alder reaction. Nature. **531**, 88–91 (2016)
19. Oancea, D., Raducan, A.: Solvent effect on ion-molecule reactions: from solution to gas phase kinetics. Rev. Roum. Chim. **42**, 849–854 (1997)
20. Kebarle, P., Dillow, G.W., Hirao, K., Chowdhury, S.: Solvation energies of ions and ionic transition states from studies of gas-phase ion–molecule reactions and equilibria. Faraday Discuss. **85**, 23–35 (1988)
21. Hagberg, D., Brdarski, S., Karlström, G.: On the solvation of ions in small water droplets. J. Phys. Chem. B. **109**, 4111–4117 (2005)
22. Vaitheeswaran, S., Thirumalai, D.: Hydrophobic and ionic interactions in nanosized water droplets. J. Am. Chem. Soc. **128**, 13490–13496 (2006)
23. Badu-Tawiah, A.K., Campbell, D.I., Cooks, R.G.: Accelerated C–N bond formation in dropcast thin films on ambient surfaces. J. Am. Soc. Mass Spectrom. **23**, 1461–1468 (2012)
24. Wei, Z., Wleklinski, M., Ferreira, C., Cooks, R.G.: Reaction acceleration in thin films with continuous product deposition for organic synthesis. Angew. Chem. Int. Edit. **56**, 9386–9390 (2017)
25. Müller, T., Badu-Tawiah, A., Cooks, R.G.: Accelerated carbon-carbon bond-forming reactions in preparative electrospray. Angew. Chem. Int. Edit. **51**, 11832–11835 (2012)
26. Takáts, Z., Wiseman, J.M., Gologan, B., Cooks, R.G.: Electrosonic spray ionization. A gentle technique for generating folded proteins and protein complexes in the gas phase and for studying ion−molecule reactions at atmospheric pressure. Anal. Chem. **76**, 4050–4058 (2004)
27. Claridge, T.D.: High-Resolution NMR Techniques in Organic Chemistry, 3rd edn. Elsevier, Oxford (2016)
28. Pritchard, J.G., Siddiqui, I.A.: Studies on the reaction of aromatic bases with epoxides, and anucleophilic buffer for the acid-catalysed hydrolysis of epoxides. J. Chem. Soc. Perkin Trans. **2**, 1309–1312 (1972)
29. Taylor, G.: Disintegration of water drops in an electric field. Proc. R. Soc. Lond. A Math. Phys. Sci. **280**, 383–397 (1964)

30. Wilm, M.S., Mann, M.: Electrospray and Taylor-cone theory, Dole's beam of macromolecules at last. Int. J. Mass Spectrom. **136**, 167–180 (1994)
31. Zhou, S., Edwards, A.G., Cook, K.D., Van Berkel, G.J.: Investigation of the electrospray plume by laser-induced fluorescence spectroscopy. Anal. Chem. **71**, 769–776 (1999)
32. Marginean, I., Parvin, L., Heffernan, L., Vertes, A.: Flexing the electrified meniscus: the birth of a jet in electrosprays. Anal. Chem. **76**, 4202–4207 (2004)
33. Duft, D., Achtzehn, T., Muller, R., Huber, B.A., Leisner, T.: Coulomb fission: Rayleigh jets from levitated microdroplets. Nature. **421**, 128–128 (2003)
34. Fallah-Araghi, A., Meguellati, K., Baret, J.C., El Harrak, A., Mangeat, T., Karplus, M., et al.: Enhanced chemical synthesis at soft interfaces: a universal reaction-adsorption mechanism in microcompartments. Phys. Rev. Lett. **112**, 5 (2014)
35. Hirabayashi, A., Sakairi, M., Koizumi, H.: Sonic spray ionization method for atmospheric pressure ionization mass spectrometry. Anal. Chem. **66**, 4557–4559 (1994)
36. Haddad, R., Sparrapan, R., Eberlin, M.N.: Desorption sonic spray ionization for (high) voltage-free ambient mass spectrometry. Rapid Commun. Mass Spectrom. **20**, 2901–2905 (2006)
37. Fenn, J.B., Mann, M., Meng, C.K., Wong, S.F., Whitehouse, C.M.: Electrospray ionization-principles and practice. Mass Spectrom. Rev. **9**, 37–70 (1990)
38. Li, Y., Cole, R.B.: Shifts in peptide and protein charge state distributions with varying spray tip orifice diameter in nanoelectrospray Fourier transform ion cycitron resonance mass spectrometry. Anal. Chem. **75**, 5739–5746 (2003)